

# Topological determination of early morphogenesis in Metazoa

Eugene Presnov · Valeria Isaeva · Nikolay Kasyanov

Received: 9 November 2008 / Accepted: 12 July 2010 / Published online: 30 July 2010  
© Springer-Verlag 2010

**Abstract** This paper presents a topological interpretation of some developmental events through the use of well-known concepts and theorems of combinatorial geometry. The organization of early embryo using a simulation of cleavage considering only blastomere contacts is examined. Each blastomere is modeled as a topological cell and whole embryo—as cell packing. The egg cleavage results in a pattern of cellular contacts on the surface of each blastomere and whole embryo, a discrete morphogenetic field. We find topological distinctions between different types of early egg cleavage and suggest a topological classification of cleavage. Blastulation and gastrulation may be related to an inevitable emergence of discrete curvature that directs development in three-dimensional space. The relationship between local and global orders in metazoan development, i.e., between local morphogenetic processes and integral developmental patterns, is established. Thus, this methodology reveals a topological imperative: a certain set of

topological rules that constrains and directs biological morphogenesis.

**Keywords** Blastulation · Cell packing · Combinatorial curvature · Convex polytope · Egg cleavage · Gastrulation · Planar graph · Structural stability · Topological polyhedra · Topological singularity

## Introduction

Obviously, spatial organization of living system is dynamic. It is also clear that living organisms inhabit and develop in the real physical space and are organized according to the properties of this space. A long time ago professor of physics Johann Benedict Listing wrote “By topology we mean the doctrine of the modal features of objects, or of the laws of connection, of relative position and of succession of points, lines, surfaces, bodies and their parts, or aggregates in space, always without regard to matters of measure or quantity” (Listing 1847). Later embryologists and scientists of high range Noel Joseph Terence Montgomery Needham and Conrad Hal Waddington noted that adequate definitions of biological morphology can be obtained through the use of topological concepts and terminology (Needham 1936; Waddington 1940). Indeed now we know from a large number of applications that topology operates with the most general properties of spaces as mathematical subjects (Bourbaki 1948). Later on, wide-ranging mathematician René Thom put forward abstract topological models of embryogenesis in his famous paper (Thom 1969). Thom always argued that quality cannot be reduced to quantity, as the discrete character of biological morphogenesis entails qualitative

---

E. Presnov (✉)  
The Volcani Center, 85280 Gilat, Israel  
e-mail: epresnov@agri.gov.il

V. Isaeva  
A.N. Severtsov Institute of Ecology and Evolution of the Russian Academy of Science, Moscow, Russia 119071  
e-mail: vv\_isaeva@mail.ru

V. Isaeva  
A.V. Zhirmunsky Institute of Marine Biology, Far East Branch of Russian Academy of Sciences, Vladivostok, Russia 690041

N. Kasyanov  
Institute of Theory of Architecture and Town Planning,  
Moscow, Russia  
e-mail: kas\_nv@mail.ru

discontinuities and involves topological relations: “there have indeed been qualitative innovations in evolution” (Thom 1969). Nowadays, the elementary topological language for formalization of biological forms and morphogenetic processes has become a more common practice and is used for simulations of form dynamics in ontogeny and evolution (Presnov 1982; Maresin and Presnov 1985; Weigel 1993; Presnov and Isaeva 1996; Jockusch and Dress 2003; Isaeva et al. 2006, 2008; Pivar 2007). The mathematical conceptions were widely explored in the past century for plant tissues and can be found in the classical monograph of D’Arcy Wentworth Thompson (1917, see Thompson 1962). Following this work, patterns of many tissues were seen as having polyhedral structures (Dormer 1980; Smolyaninov 2006). The polyhedral models became a usual approach for many problems in chemistry and physics (Atiyah and Sutcliffe 2003) as well. Our aim is to build a combinatorial scheme of embryo organization as a whole within the framework of polyhedral models.

The spatial organization of blastomeres of early embryo is a stable feature of taxonomic value, which is evolutionarily and genetically determined. During early development embryonic form creation is labile and has a variety of forms of polyhedra. These forms evolve from one to another in development. Egg cleavage can be mathematically simulated through one of the following approaches:

1. Morphological approach: transitions from stage to stage in embryo development are described based on the three-dimensional organization of blastomeres in each developmental stage. This method has a two-dimensional reduction: the conglomerate of polyhedra can be presented by projecting it on the sphere (Korn 1980; Lewis et al. 1988; Morris et al. 1989; Zarenkov 2006; de Reuille et al. 2006). Moreover, this reduction allows to formulate an epithelial topology of proliferating cells such as Markov chain (Gibson et al. 2006).
2. Functional approach: cell connections and their functions are emphasized. Each cell of the embryo is reduced to a point. Contacts between two cells are represented by line connecting the points. The dual graph for the packing cells can be build. This method also has its history in mathematical simulation of development (Mescheryakov and Belousov 1978; Doi 1984), and has evolved along with the morphological approach.

Since the present work focuses on the morphological structuring of early embryonic development, we shall firstly review some of the basic assumptions and terminology used in this field. Presumably, in the process of individual development the possible embryonic patterns do not initially possess geometrical rigidity in most animals and look sufficiently labile in this sense. All such patterns

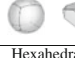
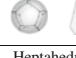



have another type of rigidity or stability, a topological one. In other words, the early patterns sequentially replacing one another are structurally stable during intervals between the topological modifications [surgeries]. For instance, differential tissues and inner cellular structures are characterized by complex external surface (Presnov et al. 1988; Poudret et al. 2008). But saying this is not enough—topology of cell connections inside embryo should also be described, because communications between neighboring cells play a crucial role during embryonic development.

To accomplish this goal, let us use some of the well-known mathematical notions. Some centuries ago Leonhard Euler proposed that all geometric patterns consist of three fundamental elements: lines [or trajectories], vertices [or crossings], and areas [or openings]. A polyhedron is a geometric figure, which is the 3d-version of the plane polygon. Put differently, it is a finite connected set of polygons joined together in such a pattern that each side of every polygon is tangent to [connected to] a side of exactly one other polygon. The cleavage embryo is a conglomerate of connected blastomeres defining the embryo’s geometry. Each blastomere has spherical external surface. This closed spherical surface of blastomere defragments into the contact domains. Let us mentally expend all these domains, so they will connect with other domains on this blastomere. We blow up each domain in such a way that it contacts with other domains on the external surface of a given cell (so for each domain its corona appears). These domains can be considered as curved faces of generalized polyhedron. Thus each blastomere looks like a non-geometrical polyhedron but a spherical polyhedron. Those polyhedra belong to class of topological polyhedra: a space homeomorphic to a polyhedron is called a topological polyhedron [t-polyhedron]. In other words we can talk about cell complex [CW-complex] as a model of biological tissue (see also Hoffman 1973; Honda et al. 2004). Any polyhedron gives rise to a graph, or skeleton, with corresponding vertices and edges. However, in case of geometric polyhedron, there must be at least 4 faces. In case of topological polyhedron, the number of faces is not restricted. Topological polyhedra appear in the beginning of the cleavage: for small blastomeric configuration. Therefore, we shall consider topological pseudo-polyhedra—spherical patterns with 1, 2, and 3 faces.



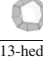


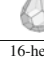
## 2d-Problems: graphs on the sphere. Polyhedral surfaces. Egg cleavage as tessellation of the sphere

Let us introduce the mathematical background of our model. A *planar graph*  $G = (V, E, F)$  is a graph which is embedded in the *Euclidean plane*  $\mathbb{R}^2$ , where  $V$  denotes the set of *vertices*,  $E$  the set of *edges* of  $G$ , and  $F$  denotes the



				
Hexahedra (8; 12; 6)	Heptahedra (10; 15; 7)	Octahedra (12; 18; 8)	Nonahedra (14; 21; 9)	Decahedra (16; 24; 10)
$4_6$ $3_4 2_5 2_2$	$4_5 5_2$ $3_2 4_3 6_2$	$4_4 5_4$ $3_4 6_4$	$4_3 5_6$ $4_6 6_3$	$4_2 5_8$ $3_4 6_6$

**Fig. 3** This figure is a continuation of previous figure. The figure presents several examples of configurations with multiple patterns on the sphere: hexahedra have 6 faces (the first is the regular one) and so on

					
Undecahedron (18; 27; 11)	Dodecahedron (20; 30; 12)	13-hedron (22; 33; 13)	Tetradecahedron (24; 36; 14)	15-hedron (26; 39; 15)	16-hedron (28; 42; 16)
$4_4 5_4 6_3$	$5_{12}$	$4_1 5_{10} 6_2$	$5_{12} 6_2$	$5_{12} 6_3$	$5_{12} 6_4$

**Fig. 4** Continuation of previous figures. Undecahedron—11 faces  $4_4 5_4 6_3$ ; dodecahedron—regular: ( $5_{12}$ ); 13-hedron—Matzke cell  $4_1 5_{10} 6_2$ . 14, 15, 16-hedrons. There are types of cells found in TCP foams (see below), each with 12 pentagonal faces like the classical regular dodecahedron ( $5_{12}$ ). The remaining three have in addition two (tetradecahedra—14 faces  $5_{12} 6_2$ ), three ( $5_{12} 6_3$ ) or four ( $5_{12} 6_4$ ) hexagonal faces, arranged antipodally, equatorially, and tetrahedrally

sphere. The configuration with five faces [ $e_2 = 5$ ] have more than 2 realizations and so on (Fig. 2).

Some spherical polyhedra in Fig. 2 have a face with 2 edges. These faces, probably, do not appear in real tissues. But these faces can be found during first egg cleavage (2-blastomere stage) for small blastomeric populations. Versions with 3 faces are not realistic for small cell packing too. When the number of faces exceeds 4, multiple solutions emerge (Figs. 3, 4).

So each configuration depicted in Figs. 2, 3, and 4 allows for many (but finite) number of different topological models of sphere packing by 2d-faces. In these figures, only some of the possible polyhedra are presented, which are the basic elements of filling constructions. In these figures, we provide standard convex polyhedra, because these many-faced polyhedra are the best models of real packing of embryonic and real tissue layers.

### 3d-Problems: space-filling by geometrical polyhedra as an example of ideal (unreal) embryonic pattern



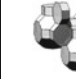
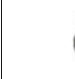
It was suggested that although the packing problem's formalism is highly suitable for embryonic cleavage, there is a substantial difference: while the former employs equal spheres, blastula cells have different dimensions (Zammataro et al. 2007). We do not intend to claim that embryonic packing can be presented by pure geometrical patterns. But we do suggest that general rules and mathematical formalization of these packing can be used in embryology. To further elaborate this suggestion, we

consider here a *locally finite* tiling of Euclidean 3d-space where each tile of the tiling is convex polytope only. A tiling of the space by polyhedra is defined as a collection of non-overlapping polyhedrons that cover the whole space without gaps: *face-to-face*. The only regular polyhedron that will produce a tiling of Euclidean 3d-space is cube, if all tiles are identical. However, obviously the cubic filling of the space is not structurally stable.

To simplify the problem, among all possible types of packing we will choose only convex polyhedra. A classic problem asks for the different types of convex polyhedra that fill the space when repeated by *translation*. In 1885, the military engineer Eugenij Stepanovich Fedorov showed that there are only five types of such packing. In one of these structures, four polyhedra meet at each vertex, three vertices are joined to four others by edges, creating a structure that chemists call a *four-connected net* (O'Keeffe 1999) and physicists—the *Plateau's laws* (here we use the term *structurally stable* instead). We will concentrate on this specific type of packing, given its structural stability.

Another property that should be considered when discussing structurally stable packing by convex polyhedra is its optimality in terms of minimization of face area under volume constraints. Lord Kelvin (Sir William Thomson) suggested that with suitably curved edges, the truncated octahedron would be the *lowest-energy* structure (that is, *lowest surface area*) of *monodisperse foam*. Kelvin believed that this polyhedron divided space into equal-volume cells with the least possible surface area. It was the first example of structurally stable packing with the simplest *periodical units* (a single *semi-regular polyhedron*)—*Kelvin 14-hedron* (or *Kelvin's cell* [tetraikaidecahedron— $4_6 6_8$ ]). Every vertex of Kelvin's cell belongs to one square face and two hexagonal faces. Kelvin's cell is the *Voronoi cell* of the *body-centered cubic lattice*. The four-connected net of edges of the configuration is the *zeolite framework* for the *sodalite structure* (zeolite framework SOD). Kelvin's cell and additional examples of periodical tiling are represented in Fig. 5, where  $A_2$  is the average number of faces per tile for 3d-tiling.

However, in 1994 it was shown, that if the foam bubbles are not required to be congruent, Kelvin's conjecture is false (Weaire and Phelan 1994). A structure with lower energy

			
$(4_6 6_8)^1$	$(4_6)^3 \cup (4_6 6_8)^1 \cup (4_6 6_8 8_6)^1$	$(4_8 8_6)^3 \cup (4_6 6_8 8_6)^1$	$(3_6 6_4)^8 \cup (3_8 8_6)^4 \cup (4_6 6_8 8_6)^4$
$4^1 6^2$	$4^3 + 4^1 6^2 + 4^1 6^1 8^1$	$4^2 8^1 + 4^1 6^1 8^1$	$3^1 6^2 + 3^1 8^2 + 4^1 6^1 8^1$
$A_2 = 14$	$A_2 = 11 \frac{2}{3}$	$A_2 = 14$	$A_2 = 14$

**Fig. 5** Space-filling tiles: body-centered cubic (BCC) lattice. *First row* is the formula of the periodic units of packing. *Second row* is the formula of vertices. *Third row* is the average number of faces per tile



was found that was based on a packing of two kinds of polyhedra. It contains eight different monodisperse cells: two regular pentagonal dodecahedra ( $5_{12}$ ) and six 14-hedra (that have twelve pentagonal faces and two hexagonal faces ( $5_{12}6_2$ )). This *Weaire-Phelan* [WP] foam is a tiling with cavities of equal volume with a considerably smaller (0.3380%) surface area than Kelvin's foam. Combinatorially, because of structural stability, foam is dual to some *triangulation* of space. This property gave rise to development of a new class of foams known as *tetrahedrally close-packed* [TCP] structures, among which is the one A15 as their counterexample to Kelvin's conjecture. In particular, it became possible to construct infinite families of new periodic TCP structures, all of which are convex combinations of the three basic TCP structures [A15, Z, and C15] (Sullivan 2000) (see corresponding periodical units on Fig. 6).

However, *real foams* often have a distribution of bubble volumes, and their topology (number of sides) is correlated with the geometry (area): larger bubbles tend to have more neighbors (Cox and Graner 2004). In non-differentiated or other tissues with dense cellular packing without extracellular matrix or cavities (embryonic 3d-tissues, fat tissue, plant meristems, and parenchyma), the geometrical similarity of cells to polyhedra is observed. The mutual compression of soft and easily deforming spherical cells having approximately equal volume results in transformation of spheres into polyhedra. In the first experimental data concerning the 3d-biological tissues were established that the average degree of cell adjacency of the elder core is close to 14 (Lewis 1943). It was found that Kelvin's cell was encountered 11 times among the randomly chosen one hundred 14-hedron cells (Hulbary 1948). Also it was constructed random monodisperse foams by individually blowing  $\sim 10^3$  bubbles and placing them into a container by hand; the most abundant cell was 13-hedron (1 quadrilateral, 10 pentagons, and 2 hexagons— $4_{15}10_{62}$ ). And it was found by studying photographs averages of 13.70 faces/cell and 5.124 edges/face (almost all faces were 4, 5, or 6 sided) but did not find any triangular faces; nor—a single Kelvin's cell (Matzke 1945).

In the course of our study of the *equal-volume* case, we encountered what we call the *kissing problem* for

(deformable) bubbles. The original kissing problem, discussed by astronomer David Gregory and Sir Isaac Newton in 1694, was “How many equal balls can touch a given ball of the same size in the same time?” In two dimensions the answer is obvious and well-known—only six hard discs can be packed around one other, in the familiar honeycomb arrangement. For the 3d-problem, consideration of the angle subtended by each sphere at the center might lead one to assume that the maximum number could be as high as 14. As it turns out, Newton was correct—the correct answer is 12 (the regular icosahedron yields a configuration of 12 touching balls (Hales 2000; Pfender and Ziegler 2004)).

### Topological tiling of the space as a real simulation of cleavage

Filling space with polyhedra is a rich source of mathematical problems, many of them still unsolved. For instance, the question of the average number of faces remains open even for the standard 3d-Euclidean space, both for geometric and topological filling (Dolbilin and Tanemura 2006). This section provides a conjecture for the average number of faces in tiles of the topological tiling problem. Let us introduce the next significations for 3d-tiling: let  $i$  be a tile;  $e_0(i)$ ,  $e_1(i)$ , and  $e_2(i)$ —be the numbers of vertices, edges, and faces of tile  $i$ . For geometrical polyhedra in 3d-Euclidean space, we have  $E_3$ —the number of polyhedra [cells]. Then summing system (1) by number of tiles [ $E_3$ ], we have for compact *three-dimensional manifold* [3-manifold] next algebraic equations:

$$\begin{cases} 3 \sum e_0(i) = 2 \sum e_1(i) \\ \sum [e_0(i) - e_1(i) + e_2(i)] = 2E_3 \end{cases} \quad (6)$$

Let  $E_0$ ,  $E_1$ ,  $E_2$ , and  $E_3$  be the numbers of vertices, edges, faces, and cells of all tiling. When abstract face-to-face tiling of 3d-space by topological polyhedra is considered, the basic property of full side contact between the faces of adjacent polyhedra remains. We can rewrite the system (6) using additional notions: for 3d-domains  $A_1$  is the average number of edges per one face in the tiling and therefore  $A_1 < 6$  since every tile is homeomorphic to sphere;  $A_2$  is the average number of faces per one cell in the tiling. By combinatorics of tiling for compact 3-manifold we have the following system:

$$\begin{cases} 4E_0 = 2E_1 \\ 4E_0 - 3E_1 + 2E_2 = 2E_3 \\ \frac{3E_1}{E_2} = A_1 \\ \frac{2E_2}{E_3} = A_2 \end{cases} \quad (7)$$

Note that  $A_2 \geq a_2$ , where  $a_2$  is the average number of faces per real tile for not compact 3d-packing with

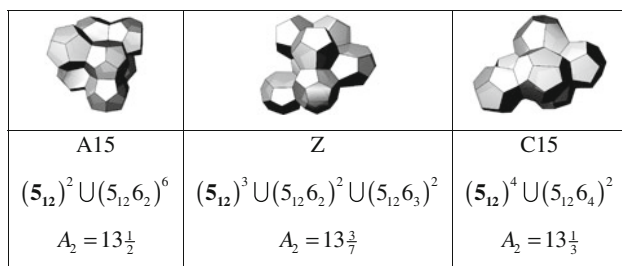


**Fig. 6** Space-filling tiles: tetrahedrally close-packed (TCP) structures

boundary. So we have the analytical expression of structural stability in 3d:

$$A_2 = \frac{12}{6 - A_1} \quad (8)$$

It is clear that  $A_1 > 4.5$  (see, for example, the analysis of regular geometrical patterns and observations in nature) and consequently from (8) we obtain  $A_2 > 8$ . The main question now is “How  $A_1$  approximates to 6?” When tiles are of equal volume in tiling, we have, probably,  $13 < A_2 \leq 14$ . How we can see from examples on Figs. 5 and 6 for periodical packing  $11\frac{3}{5} \leq A_2 \leq 14$ . Is it right for any periodical packing?

It should be noted that real physical foams or biological tissues are not compact 3-manifold. These real cell complexes always have external boundaries. Note also that the exterior of the whole embryo in this approach must be an imaginary infinite cell. This imaginary cell comes into contact with the boundaries of some blastomeres. The shape of this cell is pre-determined by the external faces of such blastomeres. So, topologically, the given foam with this imaginary cell forms compact 3-manifold. For all sets of blastomeres  $\{b^n(i)\}$  of  $n$ -blastomere stage, we have an additional *imaginary blastomere* (or blastomeres)  $\{\tilde{b}^n(n+j)\}$  with number of faces that equals  $\tilde{e}_2^n(n+j)$  (9)

In the case of compact 3-manifold, we have the next restriction:

$$\sum_{i=1}^{i=n} e_2^n(i) + \sum_{j=1} \tilde{e}_2^n(n+j) = 2m \quad (10)$$

Our conjecture for the average number of faces in specific tiles during early development is:

$$A_2 = \text{avg}\{e_2^n(i), \tilde{e}_2^n(n+j)\} \xrightarrow{[n \rightarrow N]} \text{const} < 14 \quad (11)$$

We think that this number from interval (11, 14) has stable taxonomic characteristic for each tissue in development.

Another factor to be considered is the blastomeres' shapes, which can be highly complex, with concave, flattened and convex surfaces. Blastomeres also differ in size and volume (Tassy et al. 2006). For example, a large conglomerate of connecting cells with the same number of contacts has 12 contacts per cell for not-solid tissue and 14 contacts per cell for solid tissue. When the number of contacts is smaller, for example, less than 12, the cell will be smaller in size. As a rule, cells with a large number of faces (>14 contacts) tend to have large *metrical* contributions, whereas cells with fewer faces (<12) tend to have smaller metrical contributions (Rios and Glicksman 2007).

But the average of all cells have about 12–14 contacts per cell. Moreover, big cells and therefore, cells with a large number of contacts, presumably define certain morphogenetically active centers. Therefore, inhomogeneous structures of tiling are a way to construct different tissues. The role of topological patterns in embryo decreases at further developmental stages and detailing of geometrical form takes place in organisms. Nevertheless, the prevailing of geometrical details over topological ones during organogenesis does not mean that purely topological features vanish. Thus, on the subcellular level the structural organization always depends to a high degree upon topological patterns. It is natural to assume that the geometrical variability in the whole and the topological stability of intracellular structures in particular is more characteristic of embryonic and cambial cells than of differentiated ones. When the tissue organization of multicellular plants and especially animals appears, the topological structure becomes more rigid and unified with geometrical variability of cellular packing in tissues.

A model based on cell contact number can be built for simulation of blastula formation from morula. A cell conglomerate has a set of inner contacts between blastomeres. This set of contacts is inhomogeneous. The cells do not maintain a large number of contacts or a big size in development. Big cells are not stable and thus they divide into smaller cells. Increasing number of cells during early cleavages leads also to the increasing number of contacts per cell and subsequent differentiation. Evidently, in early development, the average number of contacts per cell  $a_2$  has a tendency to increase and after a stage of 14 blastomeres this average can be close to 14 (see (2)). When the number of contacts per cell is becoming larger than 12, one inner contact face which has more than 6 neighboring faces may transform into an inner cavity.

The property of convexity means that a “curvature” (see below) of each face must be positive. For cell packing, a cell with face that has more than 6 neighboring faces exists (by inhomogeneous cell divisions Presnov 1999). Mathematically, it means that the face has negative discrete curvature. But this face is also an inner face of an adjacent cell, which has a negative curvature too. Therefore, the same physical face has couple forces directed to different sides separating the cells, so it is the reason for the appearance of the blastocoel cavity. The appearance of this cavity in the development is a necessary condition for breaking the homogeneity of cell package and for the increase of external surface. This increase in surface area would increase the free energy of the system. Additionally discussion about a physical property of curvature to be a strong driving force was done for a case of formation of small phospholipid vesicles (Wang and Du 2008).

## Combinatorial classification of blastomere packing

Before we have considered the packing conglomerate with a big number (or infinity) of cells. Now we go to small cell populations. From a mechanical point of view, many cleavage patterns do not seem like stable patterns. But this cleavage architecture is dynamic and appears in development only for a short period. So these figures of cleavage provide specific ways of describing stable patterns, which appear in the end of early development. For example, the square formation is unstable and tends to slide into the stable pattern: spherical cells (soft material) form a flat line of contact with an adjoining spherical cell that presses against it (Fig. 1). Embryologist Edwin Grant Conklin in 1897 called the line which joins the two vertexes of triple contacts, the polar furrow (Conklin 1897).

For early stages of embryogenesis we have only a small number of cells and therefore we cannot have a *statically determined cell ensemble*. So we need to find a special way of mathematical description for early development. An examination of the cleavage reveals that the *synchronous cleavage* can be described by simple formalization of contacts during early development (for any abstract organism):

$$\{1\} \rightarrow \left\{ \underline{2}, \underline{2} \right\} \rightarrow \left\{ \underline{2}, \underline{4}, \underline{4}, \underline{2} \right\} \rightarrow \left\{ \underline{3}, \underline{4}, \underline{3}, \underline{5}, \underline{4}, \underline{6}, \underline{5}, \underline{2} \right\} \rightarrow \dots \quad (12)$$

Here we need to note that this representation contains only partial information on spatial organization of embryo—we do not know which cells have contacts and can recognize only direct sisters. The first code  $\{1\}$  is the egg where the contacts are absent. The second code  $\left\{ \underline{2}, \underline{2} \right\}$  is the embryo after the first cleavage with two connected blastomeres. These two codes are universal for any organism. The third code  $\left\{ \underline{2}, \underline{4}, \underline{4}, \underline{2} \right\}$  is the result of second cleavage with 4 connected blastomeres. Next code is a set of 8 blastomeres after the third cleavage and so on. The numbers separated by comma “,” in each code is the amount of contacts of the corresponding blastomere with the neighbors and environment. More precisely the amount of contacts is the minimal number of faces (like for polyhedra, where any face is homeomorphic to a solid disk). The order of blastomeres in each code reflects the keeping order of blastomeres. The underlined pairs of numbers denote a pair that appeared as a result of the previous cleavage. Clearly, the underlined pairs will not remain in the next code. If any of the underlined pairs of blastomeres is reduced to the previous mother blastomere, then the order of the code will also return to the previous code. Thereby, genealogy of cleavage can be defined in an

algorithmic way. In the case of *asynchronous development*, the second cleavage will be as following:

$$\{1\} \rightarrow \left\{ \underline{2}, \underline{2} \right\} \rightarrow \left\{ \underline{3}, \underline{3}, \underline{3} \right\} \rightarrow \dots \quad (13)$$

Here and always we assume that only one face of the blastomere can be free from contacts with other blastomeres. For both synchronous and asynchronous cell divisions, future cleavages will lead to the combinations described above for the case of more than 4 blastomeres. Even if a blastomere does not divide (13) the amount of its contacts can be changed as a result of the cleavage. Therefore, it appears as a consequence of transition from a code to another code, which describes the transformation from one stage to another in embryo development. Up to stage of 4 blastomeres, there are 6 different consequences. If the different orders in the contacts are considered, the amount of consequences is larger.





An asynchronous cleavage is

$$\begin{aligned} \{2, 2\} &= \{(1;1;2), (1;1;2)\} \\ &\rightarrow \{3, 3, 3\} = \{(2;3;3), (2;3;3), (2;3;3)\} \\ &\rightarrow \{2, 4, 2\} = \{(2;2;2), (4;6;4), (2;2;2)\} \\ &\rightarrow \dots \end{aligned} \quad (14)$$




First case  $\{3, 3, 3\}$  is a “compact” cleavage, second  $\{2, 4, 2\}$  is a linear cleavage (Fig. 7). Here we need to use the previous notion: if external surface of cell conglomerate has some components, this cell complex will be having some *imaginary cells* (see above). This imaginary cell is like an external body that has a contact with blastomeric configuration by its whole boundary surface. So a given blastomeric configuration will be closed 3-manifold with Euler’s theorem:

$$E_0 - E_1 + E_2 - E_3 = 0 \quad (15)$$

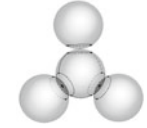
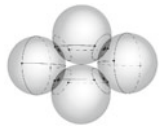

First blastomeric configurations have the following presentation (Figs. 7, 8, and 9 have the same format of ordering and the second row below blastomere’s

			
$\{1\}$ (1; 0; 1; 2) $0_1 + \tilde{0}_1$ $A_2 = 1 \quad a_2 = 1$	$\{2, 2\}$ (1; 1; 3; 3) $(1_2)^2 + \tilde{1}_2$ $A_2 = 2 \quad a_2 = 2$	$\{2, 4, 2\}$ (4; 6; 6; 4) $(2_2)^2 \cup 2_2 4_2 + \tilde{2}_2 4_2$ $A_2 = 2\frac{3}{4} \quad a_2 = 2\frac{3}{4}$	$\{3, 3, 3\}$ (2; 4; 6; 4) $(2_3)^3 + \tilde{2}_3$ $A_3 = 3 \quad a_2 = 3$

**Fig. 7** Regular stages with one, two, and three blastomeres. Combinations of single  $\{1\} = (1;0;1)$  with single imaginary cell  $\tilde{0}_1$ , two  $\{2, 2\} = \{(1;1;2), (1;1;2)\}$  with single imaginary cell  $\tilde{1}_2$ , three blastomeres  $\{2, 4, 2\}$ —three blastomeres with single imaginary cell  $2_2 4_2$  and  $\{3, 3, 3\} = \{(2;3;3), (2;3;3), (2;3;3)\}$  with single imaginary cell  $2_3$  and these constructions are structurally stable

		
$\{2, 4, 4, 2\}$ (8; 12; 9; 5) $(2_2)^2 \cup (2_2 5_2)^2 + 2_2 5_4$ $A_2 = 3\frac{3}{5} \quad a_2 = 3$	$\{4, 4, 4, 4\}$ (8; 16; 14; 6) $(2_2 4_2)^4 + (\widetilde{4_6})^2$ $A_2 = 4\frac{2}{3} \quad a_2 = 4$	$\{4, 4, 4, 4\}$ (5; 10; 10; 5) $(3_4)^4 + \widetilde{3_4}$ $A_2 = 4 \quad a_2 = 4$

**Fig. 8**  $\{2, 4, 4, 2\}$ —is linear cleavage with single imaginary cell  $2_2 5_4$ .  $\{4, 4, 4, 4\}$ —is regular cleavage with couple imaginary cells  $(\widetilde{4_6})^2$  (they give 2 additional faces) and last configuration  $\{4, 4, 4, 4\}$ : regular stages of four blastomeres:  $(3_4)^4 + \widetilde{3_4}$  is spiral cleavage with imaginary blastomere—construction is structurally stable

		
$\{2, 2, 2, 5\}$ (6; 9; 8; 5) $(2_2)^3 \cup 2_3 6_2 + 2_3 6_2$ $A_2 = 3\frac{1}{3} \quad a_2 = 2\frac{3}{4}$	$\{3, 3, 4, 4\}$ (4; 8; 9; 5) $(2_3)^2 \cup (2_2 4_2)^2 + 2_2 4_2$ $A_2 = 3\frac{2}{3} \quad a_2 = 3\frac{1}{2}$	$\{3, 3, 5, 2\}$ (6; 10; 9; 5) $(2_1 3_2)^2 \cup 2_1 3_2 5_2 \cup 2_2 + 2_1 3_2 5_2$ $A_2 = 3\frac{2}{3} \quad a_2 = 3\frac{1}{4}$

**Fig. 9** Regular stages of four blastomeres: with imaginary blastomere—construction is structurally stable

configurations is  $(E_0; E_1; E_2; E_3) = (|\text{Vertexes}|; |\text{Edges}|; |\text{Faces}|; |\text{Cells}|)$  under condition (15)).

Finally, for a synchronous cleavage up to 4-blastomere stage we found next variants:

$$\begin{aligned}
 \{1\} &\rightarrow \{2, 2\} \\
 &\quad \{2, 4, 4, 2\} - (2_2)^2 \cup (2_2 5_2)^2 \\
 &\quad \{4, 4, 4, 4\} - \langle (2_2 4_2)^4 \\
 &\quad \quad (3_4)^4 \\
 &\rightarrow \{2, 2, 2, 5\} - (2_2)^3 \cup 2_3 6_2 \\
 &\quad \{3, 3, 4, 4\} - (2_3)^2 \cup (2_2 4_2)^2 \\
 &\quad \{3, 3, 5, 2\} - (2_1 3_2)^2 \cup 2_1 3_2 5_2 \cup 2_2 \\
 &\rightarrow \dots
 \end{aligned} \tag{16}$$

Linear combinations  $\{2, 4, 4, 2\}$  and both  $\{4, 4, 4, 4\}$  are described as following Fig. 8.

The case  $\{4, 4, 4, 4\}$  has an additional topological realization—the spiral cleavage with single imaginary blastomere  $\widetilde{3_4}$ . Other patterns—irregular cleavage  $\{2, 2, 2, 5\}$  with single imaginary blastomere  $2_3 6_2$ ; rhombic cleavage  $\{3, 3, 4, 4\}$  + single imaginary blastomere  $2_2 4_2$ ; T-shaped cleavage  $\{3, 3, 5, 2\}$  + single imaginary blastomere  $2_1 3_2 5_2$  (Fig. 9).

## Discrete curvature of embryonic tissues

Here we begin an investigation of a big cell ensemble by statistics. These cell conglomerates appear during embryonic tissue formation. Returning to polyhedral surfaces we understand that sometimes it is useful to have a notion of combinatorial curvature, independent of all geometrical information (Sullivan 2008). In hexagonal 2d-cell network, presence of faces with another number of sides can be considered as a *topological dislocation of homogeneous graph* (Duvdevani-Bar and Segel 1994; Rivier et al. 2005). The non-hexagonal faces on the sphere (called *defects* or *disclinations*) appear to form 12 “scars” (or sometimes “buttons”) roughly centered at the vertices of an inscribed icosahedron. The point energies are nearly equal for a lot of “hexagonal points”, while the “pentagonal points” have relatively elevated energies and the “heptagonal points” have relatively lower energies. The appearance of non-hexagonal faces is not surprising, since an Euler’s characteristic computation readily implies that the sphere cannot be covered by hexagons alone. But what is fascinating is that the twelve formations of these five and seven nearest neighbor points appear to be independent, for example, of the ground potential (Hardin and Saff 2004).

For each graph on the sphere  $\mathbb{S}^2$  a face can be characterized by the number of neighboring faces, and discrete curvature can be also defined for polyhedral surface with canonical *Euclidean metrics* for 3d-space. We now give a general definition of polyhedral manifolds; this leads to another interpretation of *Gauss’s curvature* for a polyhedral surface. A polyhedral 3-manifold  $\mathbb{P}^3$  means a CW-complex which is *homeomorphic* to a 3-manifold, and which is regular and satisfies the intersection condition. That is, each cell is embedded in  $\mathbb{P}^3$  with no identifications on its boundary, and the intersection of any two cells (of any *dimension*) is a single cell (if it is *nonempty*). Because  $\mathbb{P}^3$  is topologically a manifold, each face is contained in exactly two cells [face-to-face].

The idea how to define a *combinatorial curvature* was presented in our previous work (Presnov and Isaeva 1990) in a simple way: on the surface of fertilized and cleaving egg ( $\mathbb{S}^2$ ) the *discrete morphogenetic field* emerges as a pattern of blastomere contacts. For every face  $f$ , a value  $k(f)$  of combinatorial curvature of this face

$$k(f) := 1 - \frac{|f|}{6} \tag{17}$$

can be defined. This is combinatorial curvature of a face on the 3d-cell, as can be understood if we apply the Gauss–Bonnet’s theorem for sphere



$$\frac{1}{2\pi} \int_{S^2} k d\sigma = 2 \quad (18)$$

Here  $k$  is *Gaussian curvature* (Dubrovin et al. 1992). With the consequence of Euler's theorem for structurally stable graphs on the sphere,  $\sum_f k(f) = 2$  (see (1)). Therefore,  $k(f)$  is the discrete analogue of continuous value  $k$ .

**Remark** The same approach was proposed elsewhere. A *corner* of a tessellating graph is a pair  $(v, f) \in V \times F$  such that  $v \in \partial f$ . The set of all corners of  $G$  is denoted by  $C := C(G)$ . Let  $G$  be a plane tessellation. Then the function  $C \rightarrow \mathbb{R}^1$  defined by

$$k(v, f) := \frac{1}{|v|} + \frac{1}{|f|} - \frac{1}{2} \quad (19)$$

is called the *combinatorial curvature* (on the graph  $G$ ) (Klassert et al. 2006). The graph  $G$  is said to have nonpositive curvature if  $k(v, f) \leq 0$  for every  $(v, f) \in C$ . In the case of planar graph (exactly for polyhedron) we can define a combinatorial curvature of vertex by next formula (Baues and Peyerimhoff 2001; Higuchi 2001; Klein 2002):

$$k(v) = \sum_{f: v \in \partial f} k(v, f) \quad (20)$$

By analogous (dual) formula we can define a combinatorial curvature of face (Higuchi 2001; Gromov 1987):

$$k(f) = \sum_{v: v \in \partial f} k(v, f) \quad (21)$$

It is easy to see that for structurally stable graph  $[|v| = 3]$  formula (21) is exactly the formula (17). Evidently, the sums of combinatorial discrete curvatures for the whole surface of a given polyhedron are calculated by different ways, which are equal:

$$\sum_f k(f) = \sum_v k(v) \quad (22)$$

For the sphere this sum equals 2 (see above Gauss–Bonnet's theorem). The definition of combinatorial curvature is relevant for planar graphs only.

### Topological conjecture about blastulation and gastrulation

The egg cleavage results in a pattern of cell contacts on the surface of the embryo as a discrete morphogenetic field. The epithelization of the primary germ layer and the progressive switch from a maternal to a zygotic control of embryo patterning takes place at different stages according

to the species. The connectivity of an epithelial layer during epithelial morphogenesis is ensured by the system of specialized intercellular contacts that integrate cells and cell cytoskeleton into a united morphological and functional entity (Kolega 1986; Zallen 2007). Epithelial cell sheets are capable for morphogenetic movements, and topological inhomogeneities presumably can determine the localization and direction (inside or outside) of the movement.

There are only five homogeneous ( $k = \text{const}$ ) discrete fields on the sphere, which correspond to five *regular polyhedra*, and only three of them are structurally stable (3<sub>4</sub>, 4<sub>6</sub> and 5<sub>12</sub> see previous figures). During synchronous cleavage divisions, only the first four blastomeres can create a *homogeneous field* on the embryo surface, later the field pattern of cellular contacts on the embryo surface inevitably becomes topologically *inhomogeneous*. As soon as the sum of adjacent faces becomes more than 6, the face's curvature becomes negative, which leads to invagination. When the number of adjacent faces is less than 6, the face's curvature is positive, which leads to evagination (see Figs. 10, 11, and 13).

An active epithelial morphogenesis was revealed in experiments in vitro: starfish eggs denuded of the fertilization membrane formed a cell monolayer after several cleavages, the cell sheets became concave, folded, and finally its edges closed forming a hollow sphere resembling

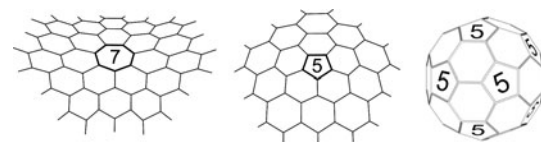


**Fig. 10** Topological inhomogeneities of surface *discrete fields*

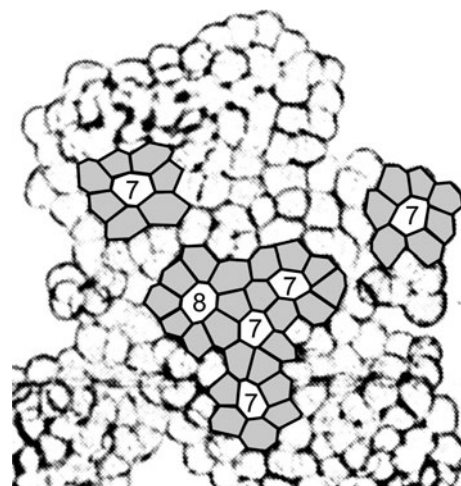


**Fig. 11** Topological inhomogeneities in monolayer of starfish blastomeres in the beginning of *blastulation* process

a normal blastula; such morphogenetic process was named blastulation (Dan-Sohkawa and Fujisawa 1980; Kadokawa et al. 1986). Figure 11 shows the modified image of a fragment from the photograph (Figure 1a) published by (Kadokawa et al. 1986); here are several cells having contacts more than 6 (i.e., negative curvature) indicated. Thus, the presence of the cells with negative curvature determines (at least, correlates with) the incurvation of the cell sheet.

We observed similar blastulation process in experiments with dissociated blastomeres using embryos of the sea urchin *Strongylocentrotus nudus*. It was shown earlier that sea urchin embryos formed from reaggregated blastomeres are possible to develop into larvae (Giudice 1962) and transform after metamorphosis into fertile sea urchins (Hinegardner 1975).

Epithelial cell layers in metazoan organisms are characterized by outer-inner anisotropy. Two sides of a cell sheet may also differ in number of cells and cell contacts (Fig. 12) that can determine the vector of an epithelial morphogenesis: incurvation (invagination) or excurvation (evagination) of the cell layer.

Topological inhomogeneities of discrete fields of cell contacts on the surface of animal and vegetative semi-spheres of cleaving embryos are demonstrated by Fig. 13. This figure represents modified images which reproduce with precision the original pattern of cell contacts between blastomeres of an annelid embryo (a, b) after (Child 1900),

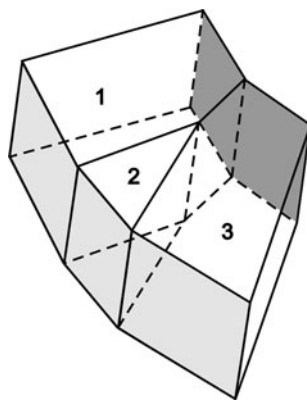


**Fig. 12** A schematic sketch illustrating a different number of cell contacts on outer and inner sides of an epithelial layer

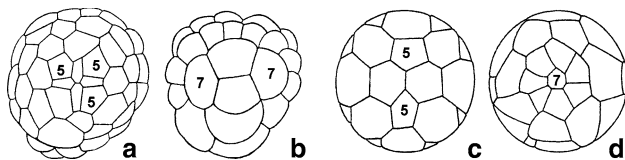


**Fig. 13** Topological singularities on the surface of animal (a, c) and vegetative (b, d) semi-spheres of cleaving embryos: a, b—*Arenicola* (Annelida); c, d—*Holopedium* (Crustacea)

and a crustacean embryo (c, d) after (Anderson 1973). The localization of the singularities of negative curvature on vegetative surface of these embryos coincides with the site of invagination during the following gastrulation process, whereas cells of positive curvature are present on the animal pole surface. Other examples of negative curvature singularities on vegetative semi-spheres of cleaving embryos in variety of animals were shown earlier (Presnov and Isaeva 1991). This means that the symmetry of the discrete morphogenetic field is breaking. The occurrence of inhomogeneity of discrete field patterns on a sphere is a consequence of the topological construction of our 3d-physical space. This rises from Euler's theorem for polyhedra. So, in accordance with biological terminology, *positional information* for discrete morphogenetic fields is determined by the Gauss–Bonnet's theorem and by Euler's theorem as a relationship between its *local order* and the *integral order*.

Obviously, gastrulation is not genetically related to the inhomogeneities of the blastomere pattern following cleavage. Rather, the place on the egg surface with the highest value of the cell field coinciding with the localization of invagination (or cell immigration), during gastrulation determines the initiation of morphogenetic cell movement (Presnov and Isaeva 1991). Conversely, cells with lowest number of contacts become centers of evagination and proliferation; a similar concept was previously put forward by (Pyshnov 1980) to explain cell proliferation in intestinal macrovilli; cells of positive curvature were actually found on the macrovillus top surface (Pyshnov 1980; see also Klein 2002; Rumpler et al. 2008). Gastrulation is the inevitable topological transition from the sphere with *field singularities* to the *torus* with homogeneous field, a transition that means zeroing of the field (Isaeva et al. 2006). The epithelial surface of an embryo after gastrulation or a larva with a through intestine tube (having both oral and anal openings) is a surface of genus 1, topologically equivalent to a sphere with one handle or to a torus. So a postgastrulation embryo or larva is a topologically stable object and, consequently, gastrulation is indeed a way of topological stabilization in embryogenesis.

Metazoan morphogenesis may be represented as a succession of shape transformations, topological modification(s) of smooth closed epithelial surfaces (Isaeva et al. 2008). This transition from blind archenteron to through intestine tube is the first topological transformation in metazoan development and evolution. Thus, the local topological surgery leads to the global topological modification of biological forms, as the genus of the surface is a global property. Topological dependence and topological constraints are fitted into evolutionary and genetically determined processes of embryogenesis—biological morphogenesis cannot be independent of the topological organization of physical space.

## Conclusions

Local singularities and the integral morphogenetic pattern are closely linked in a developing organism. In other words, the topological organization of physical space, taken as a whole, can provide a sketch of fundamental morphogenetic phenomena in biology, especially for discrete morphological transformations of external shapes that occur during development and evolution. The animal body surface is an interface between an organism and its environment, therefore, adaptive topological transformations of the body surface result in an enlargement of the interface so as to ensure the optimal distribution of external medium flows within an organism, better utilization of necessary nutrients and oxygen, and more complete excretion. The topological approach makes it possible to consider as a whole the succession of shape transformations of a metazoan organism in development and evolution, topological relation between local and global orders, topological dependence and topological constraints of biological morphogenesis.

## References

- Anderson DT (1973) Embryology and phylogeny in annelids and arthropods. Pergamon Press, Oxford, New York, Toronto, Sydney, Braunschweig
- Atiyah M, Sutcliffe P (2003) Polyhedra in physics, chemistry and geometry. Milan J Math 71:33–58
- Baues O, Peyerimhoff N (2001) Curvature and geometry of tessellating plane graphs. Discret Comput Geom 25:141–159
- Bourbaki N (1948) L'architecture de mathématiques. La Mathématique ou les Mathématiques? In: Les Grands Courants de la Pensée Mathématiques. Cahiers du Sud, Paris, pp 35–47
- Child CM (1900) The early development of *Arenicola* and *Sternaspis*. Wilhelm Roux' Archiv für Entwicklungsmechanik der Organismen 9:587–723
- Conklin EG (1897) The embryology of *Crepidula*, a contribution to the cell lineage and early development of some marine gasteropods. J Morphol 13:1–226
- Cox SJ, Graner F (2004) Three-dimensional bubble clusters: shape, packing, and growth rate. Phys Rev E 69:1409-1–1409-6
- Dan-Sohkawa M, Fujisawa H (1980) Cell dynamics of the blastulation process in the starfish, *Asterina pectinifera*. Dev Biol 77:328–339
- de Reuille PB, Bohn-Courseau I, Ljung K, Morin H, Carraro N, Godin C, Traas J (2006) Computer simulations reveal properties of the cell–cell signaling network at the shoot apex in Arabidopsis. Proc Natl Acad Sci USA 103:1627–1632
- Doi H (1984) Graph-theoretical analysis of cleavage pattern—graph developmental system and its application to cleavage pattern of Ascidian egg. Dev Growth Differ 26:49–60
- Dolbilin N, Tanemura M (2006) How many facets on average can a tile have in a tiling? Forma 21:177–196
- Dormer KJ (1980) Fundamental tissue geometry for biologists. Cambridge University Press, Cambridge
- Dubrovina BA, Novikov SP, Fomenko AT (1992) Modern geometry—methods and applications, part I: the geometry of surfaces, transformation groups, and fields. Springer-Verlag, New York
- Dubrovina BA, Fomenko AT, Novikov SP (1995) Modern geometry—methods and applications, part II: the geometry and topology of manifolds. Springer-Verlag, New York
- Duvdevani-Bar S, Segel L (1994) On topological simulations in developmental biology. J Theor Biol 166:33–50
- Gibson MC, Patel AB, Nagpal R, Perrimon N (2006) The emergence of geometric order in proliferating metazoan epithelia. Nature 442:1038–1041
- Giudice G (1962) Restitution of whole larvae from disaggregated cells of sea urchin embryos. Dev Biol 5:402–411
- Gromov M (1987) Hyperbolic groups, in Essays in group theory. Springer, New York, pp 75–263
- Hales TC (2000) Cannonballs and honeycombs. Notices Am Math Soc 47:440–449
- Hardin DP, Saff EB (2004) Discretizing manifolds via minimum energy points. Notices Am Math Soc 51:1186–1194
- Higuchi Y (2001) Combinatorial curvature for planar graphs. J Graph Theory 38:220–229
- Hinegardner RT (1975) Morphology and genetics of sea urchin development. Am Zool 15:679–689
- Hoffman WC (1973) A system of axioms for mathematical biology. Math Biosci 16:11–29
- Honda H, Tanemura M, Nagai T (2004) A three-dimensional vertex dynamics cell model of space-filling polyhedra simulating cell behavior in a cell aggregate. J Theor Biol 226:439–453
- Hulbary RL (1948) Three-dimensional cell shape in the tuberous roots of Asparagus and in the leaf of Rhoec. Am J Bot 35:558–566
- Isaeva V, Presnov E, Chernyshev A (2006) Topological patterns in metazoan evolution and development. Bull Math Biol 68:2053–2067
- Isaeva VV, Kasyanov NV, Presnov EV (2008) Analysis situs of spatial-temporal architecture in biological morphogenesis. In: Kelly JT (ed) Progress in mathematical biology research. Nova Science Publishers, New York, pp 141–189
- Jockusch H, Dress A (2003) From sphere to torus: a topological view of the metazoan body plan. Bull Math Biol 65:57–65
- Kadokawa Y, Dan-Sohkawa M, Eguchi G (1986) Studies on mechanism of blastula formation in starfish embryos denuded of fertilization membrane. Cell Differ 19:79–88
- Klassert S, Lenz D, Peyerimhoff N, Stollmann P (2006) Elliptic operators on planar graphs: unique continuation for eigenfunctions and nonpositive curvature. Proc Am Math Soc 134:1549–1559
- Klein DJ (2002) Topo-combinatoric categorization of quasi-local graphitic defects. Phys Chem Chem Phys 4:2099–2110
- Kolega J (1986) The cellular basis of epithelial morphogenesis. In: Browder W (ed) Developmental biology, vol 2. Plenum Press, pp 103–143
- Korn RW (1980) The changing shape of plant cells: transformations during cell proliferation. Ann Bot 46:649–666
- Lewis FT (1943) A geometric accounting for diverse shapes of 14-hedral cells: the transition from dodecahedra to tetrakaidecahedra. Am J Bot 31:74–81
- Lewis HW, Goel NS, Thompson RL (1988) Simulation of cellular compaction and internalization in mammalian embryo development. 2. Models for spherical embryos. Bull Math Biol 50:121–142
- Listing IB (1847) Vorstudien zur Topologie. Universität Göttingen, Göttingen
- Maresin VM, Presnov EV (1985) Topological approach to embryogenesis. J Theor Biol 114:387–398
- Matzke EB (1945) The three-dimensional shapes of bubbles in foams. Proc Natl Acad Sci USA 31:281–289
- Mescheryakov VN, Belousov LV (1978) Spatial organization of cleavage, in Itogi Nauki i Tehniki. In: VINITI (in Russian), Moscow, pp 1–100

- Morris VB, Dixon KE, Cowan R (1989) The topology of cleavage patterns with examples from embryos of *Nereis*, *Styela* and *Xenopus*. *Philos Trans R Soc Lond B* 325:1–36
- Needham J (1936) Order and life. Cambridge University Press, Cambridge
- O’Keeffe M (1999) Crystal structures—tiling by numbers. *Nature* 400:617–618
- Pfender F, Ziegler GM (2004) Kissing numbers, sphere packings, and some unexpected proofs. *Notices Am Math Soc* 51:873–883
- Pivar S (2007) An inconvenient theory. The origin of living structure by self-organization. Dalton Press, New York
- Poudret M, Arnould A, Comet JP, Le Gall P, Meseure P, Kepes F (2008) Topology-based abstraction of complex biological systems: application to the Golgi apparatus. *Theory Biosci* 127:79–88
- Presnov EV (1982) Classification of biological shapes. In: Zotin AI, Presnov EV (eds) *Mathematical developmental biology*. Nauka (in Russian), Moscow, pp 126–135
- Presnov EV (1999) Synchronization of cell division. *J Biol Syst* 7:213–223
- Presnov EV, Isaeva VV (1990) Positional information as symmetry of morphogenetic fields. *Forma* 5:59–61
- Presnov EV, Isaeva VV (1991) Local and global aspects of biological morphogenesis. *Speculations Sci Technol* 14:68–75
- Presnov EV, Isaeva VV (1996) Topological classification: onto- and phylogenesis. *Memorie della Societa Italiana di Scienze Naturali e del Museo Civico di Storia Naturale di Milano* 27:89–94
- Presnov EV, Malyghin SN, Isaeva VV (1988) Topological and thermodynamic structure of morphogenesis. In: Lamprecht I, Zotin AI (eds) *Thermodynamics and pattern formation in biology*. Walter de Gruyter, Berlin, pp 337–370
- Pyshnov MB (1980) Topological solution for cell-proliferation in intestinal crypt. 1. Elastic growth without cell loss. *J Theor Biol* 87:189–200
- Rios PR, Glicksman ME (2007) Topological and metrical analysis of normal grain growth in three dimensions. *Acta Mater* 55:1565–1571
- Rivier N, Miri MF, Oguey C (2005) Plasticity and topological defects in cellular structures: extra matter, folds and crab moulting. *Colloids Surf A* 263:39–45
- Rumpler M, Woesz A, Dunlop JWC, van Dongen JT, Fratzl P (2008) The effect of geometry on three-dimensional tissue growth. *J R Soc Interface* 5:1173–1180
- Smolyaninov VV (2006) Parallel structures in multidimensional networks. *Biofizika* 51:1106–1133
- Sullivan JM (2000) New tetrahedrally close-packed structures. In: Zitha P, Banhart J, Verbist G (eds) *Foams, emulsions and their applications*. Verlag MIT, Delft, pp 111–119
- Sullivan JM (2008) Curvatures of smooth and discrete surfaces, in discrete differential geometry. In: Bobenko AI, Schroder P, Sullivan JM, Ziegler GM (eds) *Birkhäuser*, Basel, pp 175–188
- Tassy O, Daian F, Hudson C, Bertrand V, Lemaire P (2006) A quantitative approach to the study of cell shapes and interactions during early chordate embryogenesis. *Curr Biol* 16:345–358
- Thom R (1969) Topological models in biology. *Topology* 8:313–335
- Thompson DW (1962) On growth and form. Cambridge University Press, London
- Waddington CH (1940) Organisers and genes. Cambridge University Press, Cambridge
- Wang X, Du Q (2008) Modelling and simulations of multi-component lipid membranes and open membranes via diffuse interface approaches. *J Math Biol* 56:347–371
- Weaire D, Phelan R (1994) A counterexample to Kelvin conjecture on minimal-surfaces. *Philos Mag Lett* 69:107–110
- Weigel D (1993) Patterning the Arabidopsis embryo. *Curr Biol* 3:443–445
- Zallen JA (2007) Planar polarity and tissue morphogenesis. *Cell* 129:1051–1063
- Zammataro L, Serini G, Rowland T, Bussolino F (2007) Embryonic cleavage modeling as a computational approach to sphere packing problem. *J Theor Biol* 245:77–82
- Zarekov NA (2006) Topology of cleavage in light of the Pierre Curie principle. *Russ J Develop Biol* 37:243–260